

Article

# Lipase B from *Candida antarctica* Immobilized on a Silica-Lignin Matrix as a Stable and Reusable Biocatalytic System

Jakub Zdarta <sup>1</sup>, Lukasz Klapiszewski <sup>1</sup>, Artur Jedrzak <sup>1</sup>, Marek Nowicki <sup>2</sup>, Dariusz Moszynski <sup>3</sup> and Teofil Jesionowski <sup>1,\*</sup>

<sup>1</sup> Institute of Chemical Technology and Engineering, Faculty of Chemical Technology, Poznan University of Technology, Berdychowo 4, 60965 Poznan, Poland; jakub\_zdarta@wp.pl (J.Z.); lukasz.klapiszewski@put.poznan.pl (L.K.); artur.jedrzak@gmail.com (A.J.)

<sup>2</sup> Institute of Physics, Faculty of Technical Physics, Poznan University of Technology, Piotrowo 3, 60965 Poznan, Poland; Marek.Nowicki@put.poznan.pl

<sup>3</sup> Institute of Chemical and Environmental Engineering, Faculty of Chemical Technology and Engineering, West Pomeranian University of Technology, Pulaskiego 10, 70322 Szczecin, Poland; dmoszynski@zut.edu.pl

\* Correspondence: Teofil.Jesionowski@put.poznan.pl; Tel.: +48-61-665-37-20

Academic Editor: David D. Boehr

Received: 24 November 2016; Accepted: 29 December 2016; Published: 31 December 2016

**Abstract:** A study was conducted of the possible use of a silica-lignin hybrid as a novel support for the immobilization of lipase B from *Candida antarctica*. Results obtained by elemental analysis, Fourier transform infrared spectroscopy (FTIR), X-ray photoelectron spectroscopy (XPS), and atomic force microscopy (AFM), as well as the determination of changes in porous structure parameters, confirmed the effective immobilization of the enzyme on the surface of the composite matrix. Based on a hydrolysis reaction, a determination was made of the retention of activity of the immobilized lipase, found to be 92% of that of the native enzyme. Immobilization on a silica-lignin matrix produces systems with maximum activity at pH = 8 and at a temperature of 40 °C. The immobilized enzyme exhibited increased thermal and chemical stability and retained more than 80% of its activity after 20 reaction cycles. Moreover immobilized lipase exhibited over 80% of its activity at pH range 7–9 and temperature from 30 °C to 60 °C, while native *Candida antarctica* lipase B (CALB) exhibited the same only at pH = 7 and temperature of 30 °C.

**Keywords:** silica-lignin matrix; lipase; immobilized enzymes; enzyme activity and stability

## 1. Introduction

Immobilization is commonly used as an effective tool for improving the stability and catalytic properties of enzymes [1,2]. Immobilization allows for enhancing the purity of the bounded enzyme, as well as its selectivity [3–5]. Moreover, the form of the enzyme is changing from homogenous into heterogenous after immobilization, making separation of the biocatalysts from the reaction mixture easier [6]. Binding of the biomolecules to the solid support results in the creation of the interactions that may increase rigidity and support stabilization of the tertiary and quaternary structures of the protein [7,8]. Thus, denaturation and deactivation caused by negative effects of the inhibitors and harsh reaction conditions are reduced [9,10].

The most commonly immobilized enzymes are lipases—proteins of the hydrolase group responsible for a wide range of processes of hydrolysis and transesterification of compounds of various kinds [11–13]. In this process use is made of a wide range of supports, of both organic and inorganic origin, to which the protein is attached in order to improve its properties [14,15].

In the case of lipase immobilization, special attention is paid to the hydrophobic carriers, mainly modified and unmodified polymers [16]. In hydrophobic conditions, at the organic-aqueous interface, an increase in the lipase activity is observed and this phenomenon is called interfacial activation [17]. Under these conditions, the oligopeptide lid covering the active center of the lipase undergoes rearrangements, making catalytic sites of the enzyme accessible for the substrate molecules [18,19].

Chitin is commonly used as a support for the immobilization of lipases. Due to the properties and wide availability of this material, it has been used in the immobilization of porcine pancreatic lipase. It has been shown that attaching the enzyme to the chitin surface produces systems with increased thermal and chemical stability [20]. A suitably prepared chitin matrix has also been used to immobilize the lipase from *Candida rugosa*. The resulting immobilized protein systems performed well in non-conventional biocatalysis, and may find applications in fields including advanced chemical synthesis and pharmaceuticals [21].

Another nontoxic biopolymer support is chitosan, a derivative of chitin with similar properties. The replacement of acetyl with amino groups makes this compound an attractive support for the immobilization of lipases. Rattanaphra and Srinophakun [22] used chitosan as a support to immobilize lipase. They tested their products in the transesterification of both sunflower and jatropha oil with methanol, finding that the transformation of sunflower oil is activated more easily by immobilized lipase.

With respect to inorganic supports, it is becoming increasingly popular to exploit the magnetic properties of magnetite. These features make separation of the catalyst from the reaction environment easier. Wang et al. [23] combined these properties with those of chitosan, using such a material for the immobilization of lipase from *Thermomyces lanuginosus*. This is a cheap and effective way to obtain stable systems with immobilized lipase. Chen et al. [24] used amine-functionalized Fe<sub>3</sub>O<sub>4</sub>-C nanoparticles, while Hou et al. [25] used magnetic-graphite composite nanosheets for lipase immobilization. Analysis showed that such systems have high catalytic ability.

However, the most commonly used inorganic support for lipase, as well as other enzyme immobilization is silica [26–29]. A lipase immobilized on magnesium silicate hydrate (MSH) has been used for selective esterification of conjugated linoleic acid isomers with ethanol [30]. Another type of silica, SBA-15, was modified by ionic liquids and used for lipase immobilization [31]. In that research it was analyzed how the pore size of SBA-15 silica affects the immobilization process and the properties of the resulting systems [32]. It was found that all of the silica materials used perform very well as supports for the immobilization of biocatalysts, and the resulting systems exhibit increased stability and a high level of hydrolytic activity.

To increase the chemical functionality of silica, it was decided to combine it with lignin—an interesting biopolymer which is a by-product of paper production, and has an average molecular mass of 10,000 u [33,34]. An attempt was made to combine the good adsorption properties and high stability of silica with those of lignin (a biopolymer of organic origin) in order to create a biocompatible material with high affinity to proteins, and to use it for the first time to immobilize lipase. The presence of numerous functional groups in the lignin molecule, especially hydroxylic, carboxylic, and phenolic groups on its surface, make it ideal for the selective adsorption of peptides. Due to the presence of various groups, complementary with functional groups present in the peptide structure, lignin has a good affinity for the peptides that allow for effective binding. In the present work, lipase type B from *Candida antarctica* was immobilized on the surface of silica-lignin hybrid. This is an innovative study, having the aim of producing systems of immobilized enzymes with potential applications in processes of esterification and transesterification. This work is related to our previous work on the use of a chitin-lignin material as a matrix in enzyme immobilization [35]. However, in the present study we perform a wider spectrum of analysis (including AFM and porous structure characteristics), and the effects of storage time, pH and temperature on the catalytic properties of the immobilized enzyme are examined in detail. The kinetic characteristics of the immobilized lipase are also determined.

## 2. Results and Discussion

### 2.1. Porous Structure Characterization

Determination of the parameters of the porous structure (BET surface area, total volume and mean size of pores) of the silica-lignin matrix provides indirect information about the material's sorption properties. The same parameters were determined for the systems following immobilization, formed after different process times using enzyme solutions of variable concentration. The values obtained are given in Table 1. However it should be mentioned that measurements were made under dry conditions and may differ in comparison with the results obtained under wet conditions.

**Table 1.** Porous structure parameters of silica, silica-lignin matrix, and of the products following immobilization.

Immobilization Time	Enzyme Solution Concentration (mg/cm <sup>3</sup> )	Porous Structure Characterization		
		BET Surface Area (m <sup>2</sup> /g)	Total Volume of Pores (cm <sup>3</sup> /g)	Mean Size of Pores (nm)
	Silica	262	0.12	3.84
	Silica-lignin matrix	194	0.09	2.72
1 min	0.5	161	0.08	2.46
1 h		157	0.07	2.41
24 h		155	0.07	2.21
1 min	1.0	159	0.07	2.42
1 h		152	0.06	2.23
24 h		147	0.05	2.14
1 min	3.0	147	0.05	2.39
1 h		145	0.05	2.26
24 h		140	0.05	2.09

The silica-lignin matrix has a defined porous structure with average pore size 2.72 nm, total pore volume 0.09 cm<sup>3</sup>/g, and surface area 194 m<sup>2</sup>/g. These facts stay in agreement with previously published results related to the synthesis of the silica-lignin hybrid [36,37]. The immobilization process causes small changes in both the size of the pores and the porous structure of the support, leading to a reduction in the pore size and pore volume parameters, which might be explained by the immobilization of a small amount of the enzyme in the silica pores, as well as significant changes in the surface area of the products, which provides indirect evidence of the effective deposition of the enzyme [38,39]. The greatest differences in values between the products and the matrix, notably a reduction in surface area by more than 50 m<sup>2</sup>/g, were recorded for the system obtained following an immobilization process lasting 24 h with a lipase solution of concentration 3 mg/mL.

The results confirmed the effectiveness of the immobilization, and also show that the duration of the process and the concentration of the protein solution can affect the quantity of attached protein. This observation is in agreement with results obtained by Souza et al. [40] and Gao et al. [41], who showed that prolongation of the process results in the immobilization of a greater quantity of enzyme.

### 2.2. FTIR Spectroscopy

Figure 1a shows the spectrum for the lipase B from *Candida antarctica* which underwent immobilization, and for the silica-lignin matrix. Figure 1b shows spectra for the enzyme-support systems resulting from the immobilization.

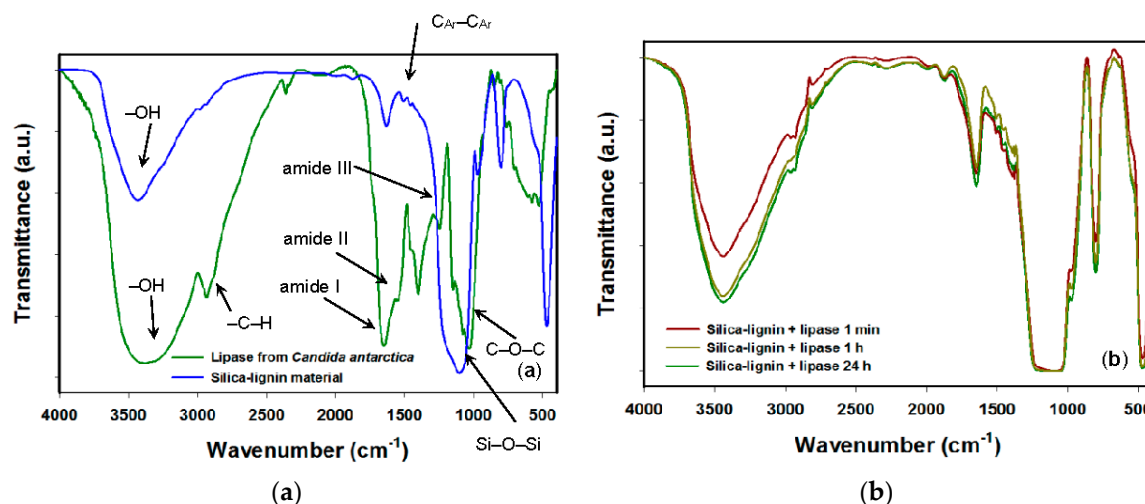


**Figure 1.** FTIR spectra of silica-lignin matrix and lipase B from *Candida antarctica* (a) and products following immobilization (b).

The spectrum for the matrix contains signals generated by chemical groups from both silica and lignin, which confirms that the hybrid material was correctly obtained. These are bands with maxima at the following wavenumbers:  $3580\text{ cm}^{-1}$  for  $\text{-OH}$  groups (stretching vibrations),  $1104\text{ cm}^{-1}$  and  $813\text{ cm}^{-1}$  for  $\text{Si-O-Si}$  groups (stretching and bending vibrations, respectively),  $968\text{ cm}^{-1}$  for  $\text{Si-OH}$  groups (stretching vibrations) and  $479\text{ cm}^{-1}$  for  $\text{Si-O}$  groups (stretching vibrations), these groups being characteristic for silica; and  $2937\text{ cm}^{-1}$  and  $2843\text{ cm}^{-1}$  for  $\text{C-H}$  bonds (stretching vibrations),  $1690\text{ cm}^{-1}$  for  $\text{C=O}$  groups (stretching vibrations),  $1610\text{ cm}^{-1}$ ,  $1517\text{ cm}^{-1}$  and  $1423\text{ cm}^{-1}$  for stretching and bending vibrations of  $\text{C}_{\text{Ar}}\text{-C}_{\text{Ar}}$  bonds and below  $1000\text{ cm}^{-1}$  for bending vibrations of  $\text{C-O}$  bonds, these being characteristic for lignin. The presence of all of these signals provides proof of the effective formation of a silica-lignin material [42].

The FTIR spectrum of the lipase B from *Candida antarctica* shows the presence of signals with maxima at the following wavenumbers:  $3480\text{ cm}^{-1}$  and  $3274\text{ cm}^{-1}$  for  $\text{-OH}$  and  $\text{-NH}$  groups (stretching vibrations),  $2936\text{ cm}^{-1}$  for  $\text{C-H}$  bonds (stretching vibrations),  $1653\text{ cm}^{-1}$ ,  $1554\text{ cm}^{-1}$  and  $1252\text{ cm}^{-1}$  for amide I, II, and III bands,  $1410\text{ cm}^{-1}$  for  $\text{-OH}$  groups (bending vibrations), and  $1146\text{ cm}^{-1}$ ,  $1080\text{ cm}^{-1}$  and  $1042\text{ cm}^{-1}$  for stretching vibrations of  $\text{C-O-C}$  bonds [43].

The FTIR analysis of the products following immobilization (Figure 1b) revealed the presence of bands at the following wavenumbers:  $3475\text{ cm}^{-1}$  for  $\text{-OH}$  and  $\text{-NH}$  groups,  $2940\text{ cm}^{-1}$  and  $2845\text{ cm}^{-1}$  for  $\text{C-H}$  bonds,  $1681\text{ cm}^{-1}$  for  $\text{C=O}$  bonds,  $1657\text{ cm}^{-1}$ ,  $1552\text{ cm}^{-1}$ , and  $1252\text{ cm}^{-1}$  for amide I, II, and III bands,  $1612\text{ cm}^{-1}$ ,  $1517\text{ cm}^{-1}$ , and  $1425\text{ cm}^{-1}$  for  $\text{C}_{\text{Ar}}\text{-C}_{\text{Ar}}$  aromatic bonds,  $1415\text{ cm}^{-1}$  for  $\text{-OH}$  groups,  $1107\text{ cm}^{-1}$  and  $815\text{ cm}^{-1}$  for  $\text{Si-O-Si}$  groups,  $969\text{ cm}^{-1}$  for  $\text{Si-OH}$  groups, and  $481\text{ cm}^{-1}$  for  $\text{Si-O}$  bonds. The presence of bands originating both from the support and from the enzyme confirms the effective immobilization of the protein on the surface of the silica-lignin matrix.

It should be noted that small changes in the intensity of peaks corresponding to particular functional groups on the spectra of the products following immobilization may suggest hydrogen interactions between the matrix surface and the enzyme [44].

### 2.3. Elemental Analysis

Table 2 contains the results of elemental analysis for the silica-lignin matrix, and also for the systems with immobilized lipase. Changes in the content of such elements as carbon, hydrogen, nitrogen, and sulfur provide an indirect indication of how the time of the immobilization process and the concentration of the enzyme solution affect the quantity of immobilized protein.

**Table 2.** Elemental composition of silica, silica-lignin materials and products following immobilization.

Immobilization Time	Enzyme Solution Concentration (mg/cm <sup>3</sup> )	Elemental Content (%)			
		C	H	N	S
	Silica	0.18	0.78	-	-
	Silica-lignin matrix	3.91	0.91	0.14	0.12
1 min	0.5	4.28	1.05	0.18	0.11
1 h		4.47	1.07	0.20	0.13
24 h		5.12	1.14	0.22	0.11
1 min	1.0	4.57	1.10	0.18	0.10
1 h		4.87	1.20	0.19	0.11
24 h		5.34	1.34	0.23	0.13
1 min	3.0	5.35	1.23	0.39	0.12
1 h		5.89	1.34	0.40	0.12
24 h		6.23	1.46	0.41	0.11

The obtained silica-lignin matrix and used in the immobilization process has a carbon content of 3.91%, a hydrogen content of 0.91%, and trace amounts of nitrogen (0.14%) and sulfur (0.12%). The data obtained are typical for this type of material, and confirm its correct preparation [36]. The presence of sulfur in the hybrid material, which does not appear directly in the composition of either of the precursors, is explained by the use of sodium sulfide in the kraft process by which lignin is obtained [37]. The small quantity of nitrogen is associated with the process of functionalization of silica with a compound from the aminosilane group to increase its affinity to the lignin surface.

The elemental composition of the systems following immobilization shows an increase in the content of carbon, nitrogen, and hydrogen in the samples, compared with the pure matrix. Occurrence of the sulfur in the samples after CALB immobilization is related both to the use of the sodium sulfide and presence of the cysteine in the structure of the lipase. This provides indirect evidence of the effectiveness of the process, because these elements are the chief components of the lipase structure [45]. The increase in the percentage content of nitrogen in the systems following immobilization is linked to its presence in the structure of the enzyme. The greatest percentage content of the elements analyzed here is found in the systems produced by immobilization lasting for 24 h from a protein solution of concentration 3 mg/mL. These results suggest that it is in these process conditions that the greatest quantity of biocatalyst is immobilized on the surface of the silica-lignin matrix, and that both parameters have an effect on the properties of the resulting systems with immobilized lipase.

#### 2.4. Atomic Force Microscopy

Atomic force microscope measurement is an effective method for obtaining surface topography. The pseudo-3D AFM images of the silica-lignin support and the product following 1 h of immobilization of lipase B from *Candida antarctica* from a solution at a concentration of 1 mg/mL are presented in Figure 2.

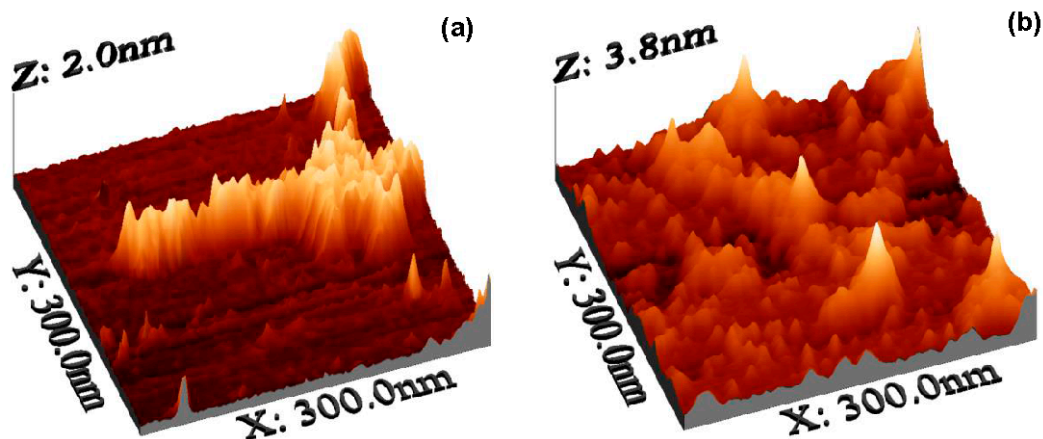


**Figure 2.** Pseudo-3D AFM images of silica-lignin matrix (a) and product following enzyme immobilization (b) for scanning at 300 nm × 300 nm.

The AFM images show significant differences in the surface morphology of the samples before and after immobilization of the lipase. The AFM results for the silica-lignin matrix show that the material has a surface with a maximum height of 2 nm. It also has a large number of pores of varying depth (0.05–0.4 nm) and diameters of about 3 nm, corresponding to the pore size diameters of a similar material obtained previously [46].

The image of the sample after immobilization of lipase B from *Candida antarctica* shows that the surface of the silica-lignin matrix is uniformly covered by the enzyme layer and the diameters of pores are much smaller than in the sample before immobilization. There are also bright points observed, at a maximum height of 3.8 nm, which may be related to the presence of the lipase molecule immobilized on the hybrid surface. These observations are similar to those previously reported by Ghosh et al. [47] and Jeyapragasam and Saraswathi [48], and fully confirm the effective immobilization of the lipase on the silica-lignin matrix surface.

### 2.5. XPS Analysis

The surface composition of the silica-lignin matrix and silica-lignin + lipase products was examined by means of X-ray photoelectron spectroscopy (XPS). Figure 3 shows the survey spectra of both analyzed materials. On the surface of the silica-lignin matrix such elements as carbon, oxygen, silicon, and sodium were identified. The surface of the silica-lignin with lipase following immobilization for 1 h from a solution of concentration 1 mg/mL, consists of all of these elements, as well as nitrogen, whose content was examined.

Surface analysis of the silica-lignin matrix confirmed that the material consists of silicon oxide (as verified by the detailed XPS Si 2p spectrum) and an organic compound with a relatively high content of carbon–oxygen bonds. The XPS C 1s spectrum of the silica-lignin matrix is very similar to that obtained for pure lignin [49]. The surface of this material is slightly contaminated by sodium and iodine atoms. The presence of these elements in the material is attributed to the lignin preparation procedure, which includes the application of iodine and sodium compounds.

Deposition of lipase onto the silica-lignin matrix results in a change in the surface composition. The fraction of silicon atoms observed on the surface is somewhat smaller than on the material before lipase immobilization. On the other hand, carbon concentration is about 50% higher. These observations are reasonable if it is considered that the enzyme is deposited onto the silica and its molecules screen part of the photoelectron signal coming from the SiO<sub>2</sub>. It is noteworthy that the iodine signal is also diminished.



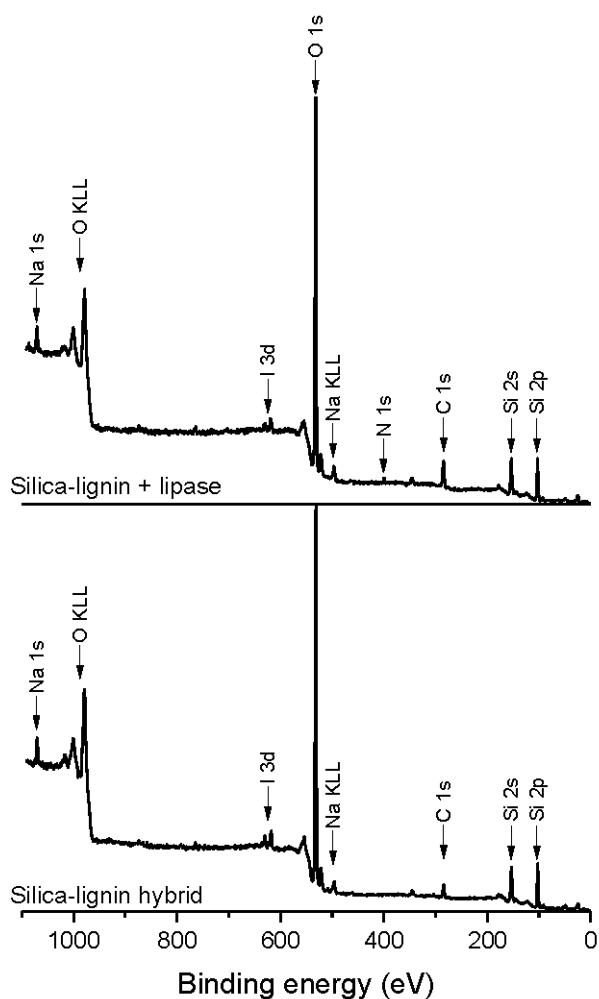


**Figure 3.** X-ray photoelectron spectra of silica-lignin matrix and silica-lignin + lipase products after immobilization.

An important piece of evidence for the successful immobilization of lipase is the additional nitrogen signal. Since the structure of lignin does not contain nitrogen atoms, the XPS N 1s signal presumably comes wholly from the lipase, which as an enzyme contains amino acids, and hence  $\text{-NH}_2$  moieties. In Figure 4 the XPS N 1s spectra from the silica-lignin + lipase system and native lipase are compared. Both spectra consist of a relatively symmetric peak located at a binding energy of 400.1 eV. The full width at half maximum (FWHM) of the XPS N 1s peak from the product after immobilization was 2.2 eV, larger than the FWHM of the peak from the pure enzyme (1.8 eV). The small difference is presumably due to the higher dispersion of lipase molecules on the surface of the silica-lignin matrix. The location of the N 1s peak is characteristic for many carbon–nitrogen and hydrogen–nitrogen bonds. According to Stevens et al. [50] the XPS N 1s line located at a binding energy of  $400.1 \pm 0.1$  eV is characteristic for amino acids and peptides. The peak is representative of the three nitrogen atoms with delocalized positive charge, as well as of amide  $\text{N-C=O}$  linkages.

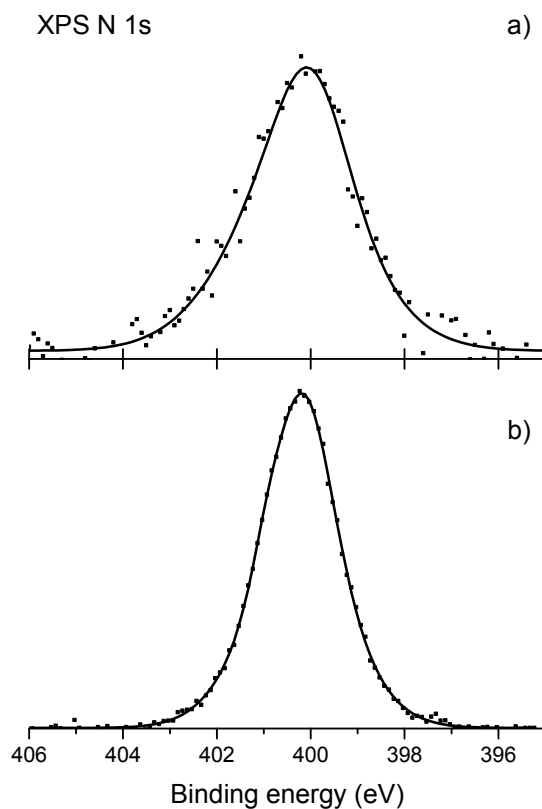


**Figure 4.** N 1s spectra of silica-lignin + lipase product after immobilization (a), and pure lipase (b).

#### 2.6. Desorption Tests of the Immobilized Lipase B from *Candida antarctica*

CALB immobilized onto the surface of the silica-lignin hybrid were incubated in the presence of 1% Triton X-100 and 0.5 M NaCl. Retention of the catalytic activity after incubation is presented in the Figure 5.

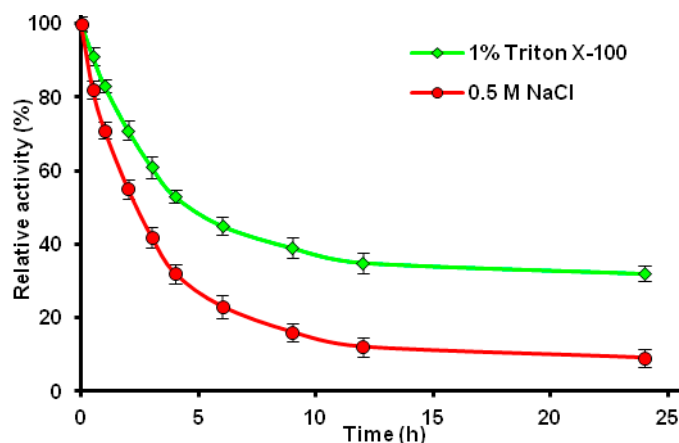


**Figure 5.** Relative activity of the lipase B from *Candida antarctica* CALB after desorption from silica-lignin support by 1% Triton X-100 and 0.5 M NaCl.

CALB immobilized onto the silica-lignin hybrid exhibit about 30% of its initial activity after 24 h of elution by Triton X-100 and less than 10% when eluted by NaCl. The lower activity noticed for the immobilized enzyme after treatment with sodium chloride suggest that CALB is bounded to the matrix via mixed adsorption. Lower activity is observed after sodium chloride treatment



as compared to the samples treated with Triton X-100 due to the fact that  $\text{Na}^+$  ions can effectively exchange CALB molecules.

However it should be noticed that the decrease in the lipase activity is mainly related to the desorption of the enzyme from the matrix, but also to the partial inactivation of the CALB caused by the presence of surfactant and inorganic salt. Moreover, according to Peirce et al., inactivated lipase may remain on the surface of the matrix, but does not exhibit catalytic activity [51].

### 2.7. Suggested Mechanism of Attachment of the Enzyme to the Silica-Lignin Matrix

Based on the results of the analysis, the authors attempted to indicate a mechanism for the attachment of the lipase to the surface of the silica-lignin matrix. The proposed mechanism of enzyme adsorption, based on the formation of hydrogen bonds, is shown in Figure 6.

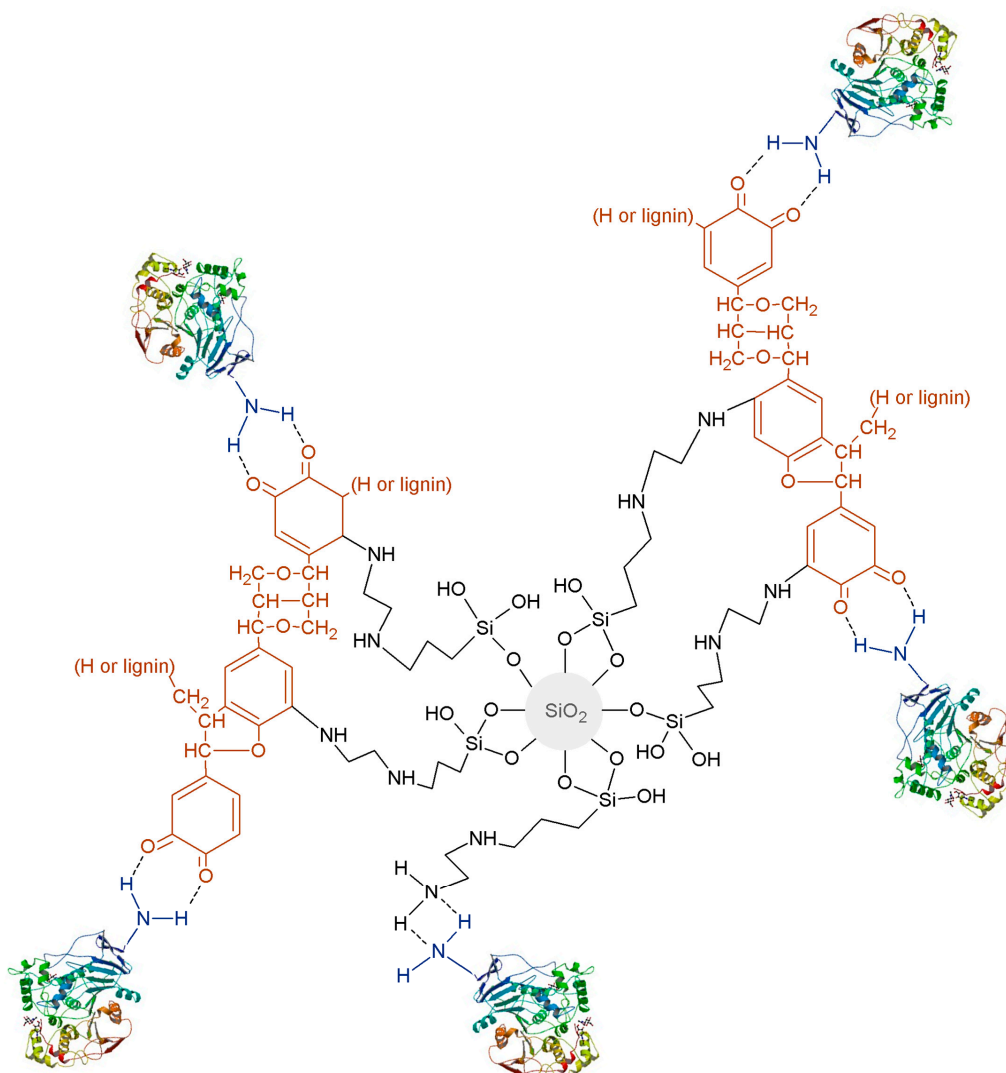


**Figure 6.** Proposed mechanism for the attachment of lipase B from *Candida antarctica* to the surface of the silica-lignin matrix.

Analysis of the test results, including FTIR, shows that the particles of the enzyme are attached to the surface of the support by means of hydrogen bonds. The presence of a significant quantity of carbonyl groups in the silica-lignin material, as well as  $-\text{NH}_2$  groups contained in the lipase structure, provide the possibility of such interactions between enzyme and matrix [52]. As a result of the process of oxidation of lignin, ortho-quinone groups are formed in its structure, as investigated by Milczarek

and Inganas [53]. Properly designed oxidation of lignin makes it possible to combine the biopolymer with silica, as we have shown in our previous studies [39,44,54]. When these interactions occur, an intermediate ring is formed, which ensures that the bonds formed are stable and makes it harder for the lipase to be washed off the surface of the support during successive catalytic cycles [55]. However, it should be noted that the presence of amino groups on the silica surface means that single particles of the lipase may attach to them instead of to the lignin, as is also shown in Figure 6.

### 2.8. Retention of Hydrolytic Activity

The catalytic activity of the immobilized and native lipase was assessed spectrophotometrically based on the hydrolysis reaction of *para*-nitrophenyl palmitate (*p*-NPP). Analysis was performed on samples obtained after different process times and using solutions of the protein at different concentrations, in order to identify the immobilized enzyme systems with the greatest retention of hydrolytic activity (Figure 7).

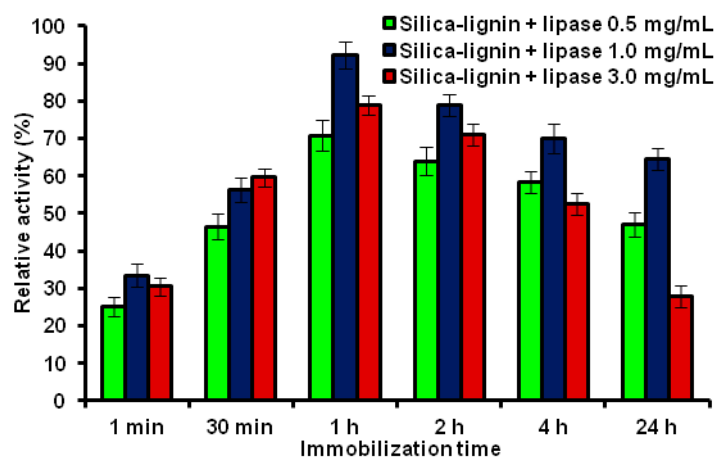


**Figure 7.** Retention of the catalytic activity of the immobilized enzymes depending on the immobilization time and the enzyme solution concentration.

The calculated hydrolytic activity of all systems after immobilization was lower than that of the native enzyme. The results clearly indicate that both time of immobilization and the concentration of the enzyme solution have a significant effect on the catalytic ability of the immobilized lipase. In the initial stages of the adsorption process larger quantities of the enzyme can be immobilized from the 3.0 mg/mL solution than from the 0.5 mg/mL solution. In fact, in the case of the 0.5 mg/mL solution, lower expressed activity is observed, which might be related to the hydrophilic/hydrophobic character of the silica-lignin material. Silica possesses mainly hydroxyl groups on its surface (hydrophilic surface properties) that can produce lipase inactivation and result in lower activity. When the concentration of the enzyme solution increased (a greater amount of the enzyme is presented in the solution) higher amounts of enzyme particles are immobilized at the more hydrophobic regions of the support (related to the presence of the lignin). In these regions interfacial activation takes place, lipase is being activated, and higher activity retention is observed [56]. Moreover, the presence of the various regions at the support structure can generate various orientation of the enzyme molecules that resulting in various catalytic activity of the immobilized biocatalysts [57]. The use of a longer process time and higher concentration of biocatalyst leads to the adsorption of larger quantities of the enzyme, which has an unfavorable impact on the catalytic properties of the products. Similar observations were made by Sheldon and van Pelt [58], who showed that significant accumulation of enzyme molecules led to the creation of aggregates and caused blocking of the active sites of the enzyme, leading to a reduction in their activity. They have also revealed that longer immobilization time may lead to the enzyme degradation caused by the process conditions. Moreover longer immobilization time and accumulation

of a greater amount of the enzyme not only blocks the lipase active center but also may induce some diffusional limitations. For enzyme solutions of lower concentration the adsorption process is slower and smaller quantities of the enzyme can be adsorbed and, hence, the observed catalytic activity for this parameter is higher. The highest retention of catalytic activity (92% of native lipase) is observed for systems formed after immobilization for 1 h using a solution of concentration 1 mg/mL. After a process carried out under these conditions, 16.72 mg of the lipase was immobilized per 1 g of the silica-lignin matrix. This value is almost five times higher than the quantity of lipase immobilized on the surface of silica by Forsyth and Patwardhan [59], which those authors claim to represent the maximum capacity of silica. Thus, combining silica and lignin into a hybrid material significantly increases the sorption capacity of the matrix in comparison with silica. The systems exhibiting the highest catalytic activity (duration of immobilization of 1 h, protein solution concentration 1 mg/mL) possess the best hydrolytic properties thus this products was, used in further analysis to determine its stability and durability.

### 2.8.1. Effect of pH

Enzymes exhibit their higher activity within a narrow pH range; hence, it is important to determine how immobilization affects the chemical stability of the biocatalyst. Figure 8 shows changes in the hydrolytic activity of the free and immobilized lipase in the pH range 3–11.

The data presented in Figure 8 show changes in the catalytic activity of native and immobilized CALB as a function of the pH of the reaction system.

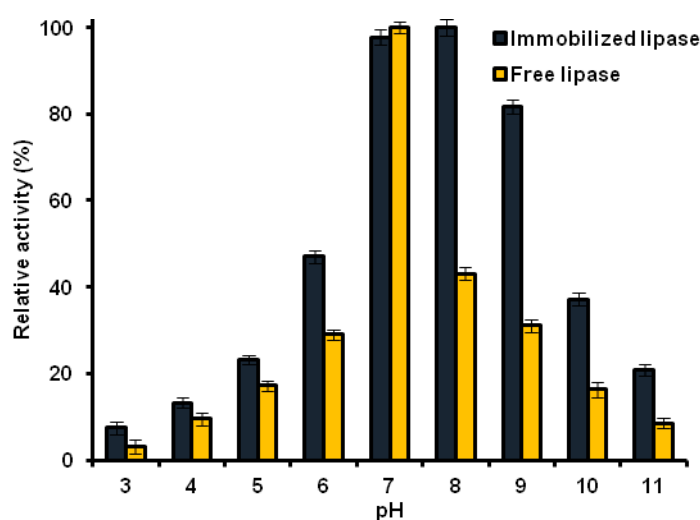
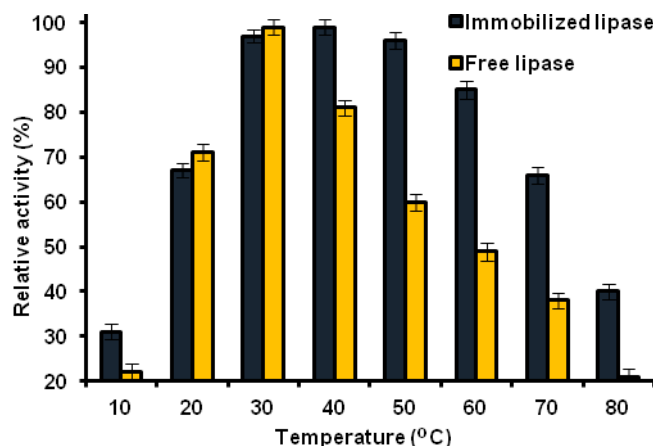


Figure 8. Effect of pH on activity of the native and immobilized lipase.

The immobilized lipase demonstrates high activity (over 80%) in the pH range 7–9, with a maximum in weakly alkaline conditions (pH = 8). Note should be made of the widening of the range of high activity of the protein when immobilized on the silica-lignin support, compared with the native enzyme, which has high catalytic ability only at pH = 7, meaning that even small changes in the chemical nature of the reaction environment cause significant changes in the activity of that biocatalyst. Experiments provided by Emregul et al. [60] and Dong et al. [61] concerning the immobilization of lipases on composite materials also indicated an increase in the pH stability of the immobilized enzyme. Matrix-bonded lipase exhibited activity of over 80% in the pH ranges 6–7 and 7.5–8, respectively. Nevertheless, the results of the present study show that lipase attached to a silica-lignin matrix exhibits even higher resistance to varying pH (activity over 80% in a pH range from 7 to 9). The increase in the chemical stability of the immobilized lipase is probably caused by conformational changes in the quaternary structure of the protein, resulting from immobilization [62].

### 2.8.2. Thermal Stability

The thermal stability of the products following immobilization is one of the most important parameters determining the possibility of using those systems in enzymatic reactions. It was determined how the temperature, in the range 10–80 °C, affects the hydrolytic activity of both the native enzyme and the immobilized product. The results are shown in Figure 9.



**Figure 9.** Thermal stability of native and immobilized lipase in the temperature range 10–80 °C.

The native lipase B from *Candida antarctica* exhibits its highest catalytic activity at a temperature of 30 °C, and increasing the temperature causes a significant reduction in the activity of the protein. The lipase immobilized on the surface of the silica-lignin matrix is most active at 40 °C, and a further rise in temperature, even by another 20 °C, does not cause a significant deterioration. A similar study, using the natural polymer sporopollenin, was conducted by Tutarb et al. [63]. Those authors described the increase in the thermal stability of the immobilized enzyme and showed that lipase exhibits over 80% of its initial activity at temperatures of 30 and 40 °C; meanwhile, the product after immobilization on a silica-lignin matrix retains more than 80% of its initial hydrolytic activity across a wide temperature range from 30 °C to 60 °C. These results show that depositing the biocatalyst on this support significantly expands the range of temperatures at which the resulting system can be used. This is probably due to the increase in the stability of the entire protein structure brought about by the immobilization of the enzyme [64], as a result of which the protein molecule does not undergo deformation and, thus, becomes more resistant to denaturation [65].

### 2.8.3. Reusability

Since the immobilization process can have a significant impact on the duration of the catalytic activity of enzymes, changes in activity over 20 catalytic cycles were determined. After each individual reaction the product with immobilized lipase was separated from the reaction mixture, washed thoroughly with phosphate buffer, and reused. The results are shown in Figure 10.

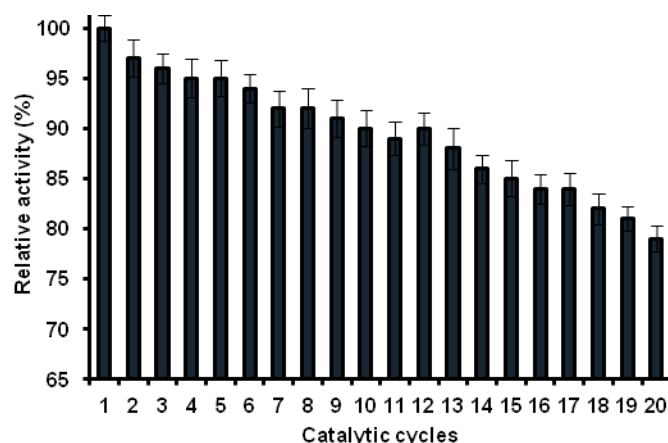


**Figure 10.** Reuse stability of lipase immobilized on the silica-lignin hybrid matrix.

The product with CALB immobilized on the silica-lignin support show only a small drop, of around 20%, in catalytic activity after 20 full reaction cycles. These results indicate that the immobilized enzyme, due to changes taking place in its molecule, retains catalytic activity for a much longer period of time. Its use may, therefore, lead to reductions in process costs [66]. The retention of a high level of activity after so many catalytic cycles may be linked to the creation of stable interactions between the lipase and the silica-lignin matrix, causing a significant reduction in the washing out of the enzyme from the surface of the inorganic-organic support. Furthermore, attachment of the protein to the solid support protects the enzyme against changes in its structure, making the whole particles more stable [67]. For the hydrolysis reaction of *para*-nitrophenyl palmitate to nitrophenol, after 20 catalytic cycles, immobilized lipase still retained 80% of its initial catalytic activity. In comparison, lipases from *Candida rugosa* and *Rhizopus oryzae* immobilized on silica gel by Ho et al. [68] preserved 80% of their initial activity after five repeated catalytic cycles. Thus, use of the silica-lignin matrix maintains the good catalytic properties of the immobilized enzyme for up to four times more reaction cycles.

#### 2.8.4. Storage Stability

The storage stability of free and immobilized enzyme, stored at 4 °C and 20 °C, was investigated as described in Section 3.4. The results are shown in Figure 11.

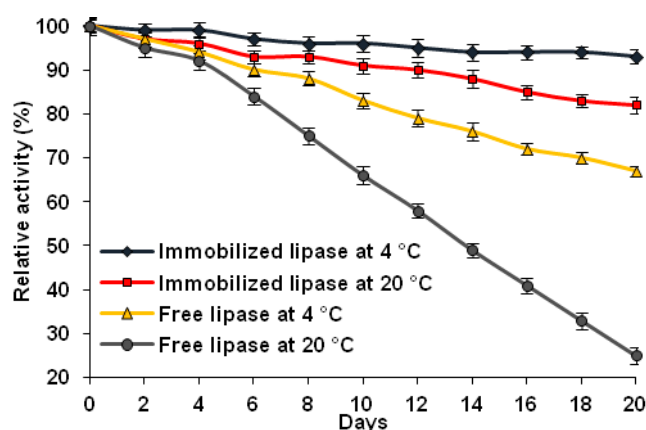


**Figure 11.** Storage stability of the free and immobilized lipase stored at 4 °C and 20 °C.

The catalytic activity of native lipase depends strongly on the storage temperature, while the free enzyme, when stored at 4 °C, retains around 70% of its original activity even after 20 days, the same protein stored at 20 °C for the same length of time retains only around 25% of its original catalytic

ability. Much better results were obtained for the products following immobilization, for which the storage stability was higher than for the native lipase, irrespective of the storage temperature. It should be noted, however, that the temperature of storage of the products following immobilization does influence their catalytic ability. The systems stored at 4 °C, after the analyzed time period, retain almost all of their original activity (96%), while immobilized lipase stored at 20 °C shows a decline in activity by approximately 10%. Chen et al. [69] reported activity of lipase immobilized on chitosan microspheres at levels of 80% and 60% after storage at 4 °C for 5 and 20 days, respectively. Meanwhile Zhu et al. [70] found that lipase immobilized on silica-coated magnetic nanoparticles preserved 70% of its initial activity after 20 days, when stored at 20 °C. The results obtained in our research indicate that immobilization of *Candida antarctica* lipase B on a silica-lignin support significantly extends its catalytic activity compared with the free enzyme and with previously published results. This fact might be explained by the protection of the three-dimensional structure of the biocatalyst which leads to preservation of the active centers intact, as a result of which high catalytic activity of the immobilized lipase is observed [71].

### 2.9. Kinetic Parameters

The Michaelis–Menten constant ( $K_m$ ) and  $V_{max}$  values were calculated based on spectrophotometric measurements according to Lineweaver–Burk plots for free and immobilized lipase.

The  $K_m$  value of the native lipase calculated for *p*-NPP was  $3.24 \pm 0.39$  mM, while for the immobilized lipase the value increased to  $4.36 \pm 0.32$  mM. This means that the immobilized lipase B from *Candida antarctica* has a lower affinity to the substrate than the native enzyme. This observation is similar to that of Wang et al. [72], and results from the fact that the immobilization process causes loss of the enzyme flexibility that is necessary for effective substrate binding. In turn, the value of  $V_{max}$  for the native enzyme is  $33.05 \pm 1.37$  U/mg, decreasing to  $29.36 \pm 1.25$  U/mg following immobilization, again, due to the lower affinity to the substrate.

## 3. Materials and Methods

### 3.1. Materials

Silica, in the form of the commercial product Syloid<sup>®</sup>244, was obtained from W.R. Grace and Co. (Columbia, MD, USA). Kraft lignin (product number 471003), *N*-(2-aminoethyl)-3-aminopropyltrimethoxysilane (97%), sodium meta-periodate (>99%), and lipase type B from *Candida antarctica* were supplied by Sigma-Aldrich (Saint Louis, MO, USA). Methanol and dioxane (laboratory grade) were purchased from Chempur Company (Gliwice, Poland). A phosphate buffer at pH = 7 was obtained from Amresco Company (Solon, OH, USA). *para*-nitrophenyl palmitate (*p*-NPP), Triton X-100 (laboratory grade), sodium chloride, and gum arabic were acquired from Sigma Aldrich (Saint Louis, MO, USA).

### 3.2. Matrix Preparation and Lipase Immobilization

The silica was modified by five parts by weight of *N*-(2-aminoethyl)-3-aminopropyltrimethoxysilane, using as a solvent methanol:water in a ratio of 4:1 (*v/v*). A detailed description of this method of modifying SiO<sub>2</sub> can be found in [73–75]. The lignin was dissolved in a mixture of dioxane and water in a ratio of 9:1 (*v/v*). An aqueous solution of sodium periodate (1.5 g in 30 mL of water) was also prepared, and this was added to the lignin solution. After the oxidizing agent had been added, the system was additionally mixed using a fast rotary mixer (Eurostar Digital (IKA Werke GmbH, Staufen im Breisgau, Germany) for 30 min in darkness. The pretreated silica was then added to the mixture, and the system was mixed for 1 h. The resulting silica-lignin hybrid material was placed in a vacuum evaporator to distill off the solvents. The product was dried in a convection dryer (Memmert, Schwabach, Germany) for 8 h at 105 °C. This process has been developed and described in detail in previously published work [43–54].



A quantity of 500 mg of the obtained silica-lignin matrix was placed in a reactor, 20 mL of a solution of the enzyme at the concentrations of: 0.5, 1.0, and 3.0 mg/mL in phosphate buffer at pH = 7 was added, and the mixture was placed on a shaker (IKA Werke GmbH, Staufen im Breisgau, Germany) for 1 and 30 min and for 1, 2, 4, and 24 h. The immobilized enzyme products were filtered under reduced pressure and dried at room temperature for 24 h.

### 3.3. Analysis of the Products Following Immobilization

In order to compare the porous structure parameters of the immobilized enzyme systems with those of the original support, surface area, total volume of pores and average pore diameter were determined using an ASAP 2020 instrument (Micromeritics Instrument Co., Norcross, GA, USA). The surface area was determined by the multipoint Brunauer–Emmett–Teller (BET) method using data for adsorption under relative pressure ( $p/p_0$ ). The Barrett–Joyner–Halenda (BJH) algorithm was applied to determine the pore volume and average pore size. For adsorptive characterization of each sample, three measurements were made. Due to the high accuracy of the instrument used, surface area was determined to an accuracy of  $\pm 0.1$  m<sup>2</sup>/g, pore volume to  $\pm 0.01$  cm<sup>3</sup>/g, and pore size to  $\pm 0.01$  nm.

The effective immobilization of the enzyme was confirmed by the results of Fourier transform infrared spectroscopy (FTIR). Measurements were made on a Vertex 70 apparatus (Bruker, Billerica, MA, USA). Substances were analyzed as tablets prepared by mixing 250 mg of anhydrous KBr with 1.5 mg of the substance. Spectra were produced over a wavenumber range of 4000–420 cm<sup>-1</sup>, with a resolution of 0.5 cm<sup>-1</sup>.

The elemental composition of the matrix and products following immobilization was determined using a Vario EL Cube instrument (Elementar Analysensysteme GmbH, Langensfeld, Germany), which enables determination of the content in a sample of such elements as carbon, hydrogen, nitrogen, and sulfur, by means of high-temperature combustion. The results are given to  $\pm 0.001\%$ , and each is obtained by averaging three measurements.

X-ray photoelectron spectra (XPS) were obtained using Al  $K\alpha$  ( $h\nu = 1486.6$  eV) radiation with a Prevac system equipped with a Scienta SES 2002 (Scienta Omicron, Taunusstein, Germany) electron energy analyzer operating at constant transmission energy ( $E_p = 50$  eV). The spectrometer was calibrated using photoemission lines (with reference to the Fermi level): EB Cu 2p<sub>3/2</sub> = 932.8 eV, EB Ag 3d<sub>5/2</sub> = 368.3 eV and EB Au 4f<sub>7/2</sub> = 84.0 eV. The instrumental resolution, as evaluated by the full-width at half maximum (FWHM) of the Ag 3d<sub>5/2</sub> peak, was 1.0 eV. The analysis chamber was evaluated during the experiments to lower than  $1 \times 10^{-9}$  mbar. Charging effects were corrected using the C 1s peak ascribed to aliphatic carbon bonds (CH<sub>x</sub>) and set to 285.0 eV. The XPS lines of other observed elements were shifted correspondingly. The reproducibility of the peak positions thus obtained was  $\pm 0.1$  eV. The surface composition of the samples was obtained on the basis of the peak area intensities using the sensitivity factor approach and assuming homogeneous composition of the surface layer.

The AFM measurements were made using an Agilent 5500 (Palo Alto, CA, USA) atomic force microscope in intermittent contact mode. BudgetSensors All-in-One type levers with a resonance frequency of about 150 kHz were used for scanning. Data analysis was performed using the WSxM software [76]. The test material was applied to a mica surface that had previously been cleaned by mechanical stripping. A spin-coating method was used for distribution of the samples on the mica.

### 3.4. Hydrolytic Activity

The hydrolytic activity of the immobilized lipase was determined based on the spectrophotometric measurements ( $\lambda = 410$  nm) made on Jasco V-750 (Oklahoma City, OH, USA) during the hydrolysis reaction of *para*-nitrophenyl palmitate (*p*-NPP) to *para*-nitrophenyl (*p*-NP) and palmitic acid, according to our previous work [39]. All reactions (performed in triplicate) were carried out with stirring at 1000 rpm at 30 °C for 2 min. For the model reaction of *p*-NPP into *p*-NP, 5 mg of the native enzyme and an appropriate amount of the product after immobilization containing 5 mg of the lipase were used. Activity retention ( $A_R$ ) after immobilization was calculated from the following equation:



$$A_R = \frac{A_I}{A_0} \times 100\% \quad (1)$$

where  $A_0$  denotes the total initial activity of the lipase, and  $A_I$  denotes the activity of the immobilized enzyme.

#### 3.4.1. Effect of pH

The effect of pH was determined based on the same hydrolysis reaction, carried out with stirring at 1000 rpm at 40 °C for 2 min. The reactions were carried out at different pH values, ranging from 3 to 11. After incubation in a buffer solution at the appropriate pH for 1 h, the activity of the products obtained was measured spectrophotometrically. For each pH the extinction coefficient have been calculated separately at 410 nm.

#### 3.4.2. Thermal Stability

Effect of the temperature on hydrolytic activity of the immobilized lipase was established using the hydrolysis reaction of *p*-NPP to *p*-NP. The reaction was carried out at constant temperature for 2 min with stirring at 1000 rpm over a temperature range from 10 °C to 80 °C at pH 8. The measurements were carried out on Jasco V-750 (Oklahoma City, OH, USA) spectrophotometer equipped with a Peltier-thermo cell holder (Oklahoma City, OH, USA).

#### 3.4.3. Reusability

Reusability was estimated based on the reaction described above. After each hydrolysis step, the immobilized enzyme products were separated from the reaction mixture by centrifugation. The biocatalyst was then washed with 30 mL of phosphate buffer and dried for 24 h at ambient temperature, and used to catalyze a further reaction cycle.

#### 3.4.4. Storage Stability

The storage stability of the native lipase and the products following immobilization was determined using the reaction described in details in Section 3.4. The hydrolytic activity after a given storage time was determined for samples stored at 4 °C and at 20 °C.

### 3.5. Kinetic Parameters

Kinetic parameters of free and immobilized lipase B from *Candida antarctica* were determined based on the reaction described in Section 3.4. The Michaelis constant ( $K_m$ ) and the maximum rate of reaction ( $V_{max}$ ) were calculated according to Lineweaver–Burk plots using the initial rate of reaction:

$$v = \frac{V_{max}[S]}{K_m + [S]} \quad (2)$$

$$\frac{1}{v} = \frac{K_m}{V_{max}} \cdot \frac{1}{[S]} + \frac{1}{V_{max}} \quad (3)$$

where  $[S]$  denotes the concentration of the substrate,  $V$  and  $V_{max}$  denote the initial and maximal rate of reaction, and  $K_m$  denotes the Michaelis–Menten constant.  $V_{max}$  is defined as the highest possible rate when all enzymes were saturated with the substrate.  $K_m$  is defined as the substrate concentration that yielded half the maximum rate of reaction, reflecting the effective characteristics of the enzyme and the affinity between enzyme and substrate, as well as diffusion effects.

#### 3.6. Desorption of the Immobilized CALB

Samples of the 500 mg of the immobilized CALB were suspended in 5 mL of 1% Triton X-100 in phosphate buffer or in 5 mL of 0.5 M NaCl solution. Samples were taken under stirring at 500 rpm.

After 30 min and 1, 2, 4, 6, 9, 12, and 24 h samples were taken, centrifuged, and the activity was determined based on the *p*-NPP hydrolysis reaction (Section 3.4).

#### 4. Conclusions

The authors have synthesized and then successfully used a functional silica-lignin matrix as a novel support for the immobilization of lipase B from *Candida antarctica*. The results of analysis, including FTIR, XPS, AFM, elemental analysis, and porous structure determination, confirmed the effective immobilization of the enzyme. These results also led to a description of a mechanism for the immobilization, based on hydrogen interactions. Sophisticated analysis was made of the catalytic activity and stability of the immobilized lipase, and the system with the highest activity retained 92% of the activity of the native enzyme. The immobilized enzyme exhibits its maximum activity at pH = 8 and at a temperature of 40 °C, while, for the native lipase, the corresponding values are pH = 7 and 30 °C. The immobilized lipase retains over 80% of its activity in the pH range 7–9 and the temperature range 30–60 °C. Moreover, this activity is also observed after 20 catalytic cycles and after 20 days of storage, irrespective of the storage conditions. The obtained system exhibits a slight decrease in the affinity of the immobilized enzyme to the substrate (higher  $K_m$  values), associated with a decrease in the maximum reaction rate ( $V_{max}$ ). The prepared materials may have applications in many processes based on esterification and transesterification reactions and in the field of advanced biosensors. Hence, further investigations related to the potential applications of the obtained systems, as well as utilization of the silica-lignin hybrid as a matrix for broad variety of the various enzymes, will be undertaken.

**Acknowledgments:** This work was supported by research grant funds from the National Science Center Poland in accordance with decision No. DEC-2013/09/B/ST8/00159.

**Author Contributions:** J.Z. Planning studies. Evaluation of enzyme immobilization efficiency and immobilized enzyme activity and stability. Results development. L.K. Preparation of functional silica-lignin biosorbent. A.J. Carried out of the immobilization experiments. M.N. Results development of the AFM. analysis. D.M. Results development of the XPS. analysis. T.J. Coordination of all tasks in the paper. Planning studies. Results development.

**Conflicts of Interest:** The authors declare no conflicts of interest.

#### References

1. Manzo, R.M.; de Sousa, M.; Fenoglio, C.L.; Barro Goncalves, L.R.; Mammarella, E.J. Chemical improvement of chitosan-modified beads for the immobilization of *Enterococcus faecium* DBFIQ E36 l-arabinose isomerase through multipoint covalent attachment approach. *J. Ind. Microbiol. Biotechnol.* **2015**, *42*, 1325–1340. [[CrossRef](#)] [[PubMed](#)]
2. Jesionowski, T.; Zdarta, J.; Krajewska, B. Enzymes immobilization by adsorption: A review. *Adsorption* **2014**, *20*, 801–821. [[CrossRef](#)]
3. Garcia-Galan, C.; Berenguer-Murcia, A.; Fernandez-Lafuente, R.; Rodrigues, R.C. Potential of different enzyme immobilization strategies to improve enzyme performance. *Adv. Synth. Catal.* **2011**, *353*, 2885–2904. [[CrossRef](#)]
4. Guzik, U.; Hupert-Kocurek, K.; Wojcieszynska, D. Immobilization as a strategy for improving enzyme properties—Application to oxidoreductases. *Molecules* **2014**, *19*, 8995–9018. [[CrossRef](#)] [[PubMed](#)]
5. Rodrigues, R.C.; Ortiz, C.; Berenguer-Murcia, A.; Torres, R.; Fernandez-Lafuente, R. Modifying enzyme activity and selectivity by immobilization. *Chem. Soc. Rev.* **2013**, *42*, 6290–6307. [[CrossRef](#)] [[PubMed](#)]
6. Barbosa, O.; Ortiz, C.; Berenguer-Murcia, A.; Torres, R.; Rodrigues, R.C.; Fernandez-Lafuente, R. Strategies for the one-step immobilization-purification of enzymes as industrial biocatalysts. *Biotechnol. Adv.* **2015**, *33*, 435–456. [[CrossRef](#)] [[PubMed](#)]
7. Hernandez, K.; Fernandez-Lafuente, R. Control of protein immobilization: Coupling immobilization and site-directed mutagenesis to improve biocatalyst or biosensor performance. *Enzyme Microb. Technol.* **2011**, *48*, 107–122. [[CrossRef](#)] [[PubMed](#)]
8. Secundo, F. Conformational changes of enzymes upon immobilisation. *Chem. Soc. Rev.* **2013**, *42*, 6250–6261. [[CrossRef](#)] [[PubMed](#)]

9. Fernandez-Lafuente, R. Stabilization of multimeric enzymes: Strategies to prevent subunit dissociation. *Enzyme Microb. Technol.* **2009**, *45*, 405–418. [[CrossRef](#)]
10. Cowan, D.A.; Fernandez-Lafuente, R. Enhancing the functional properties of thermophilic enzymes by chemical modification and immobilization. *Enzyme Microb. Technol.* **2011**, *49*, 326–346. [[CrossRef](#)] [[PubMed](#)]
11. Khoobi, M.; Motevalizadeh, S.F.; Asadgol, Z.; Forootanfar, H.; Shafiee, A.; Faramarzi, M.A. Synthesis of functionalized polyethylenimine-grafted mesoporous silica spheres and the effect of side arms on lipase immobilization and application. *Biochem. Eng. J.* **2014**, *88*, 131–141. [[CrossRef](#)]
12. Lima, L.N.; Oliveira, G.C.; Rojas, M.J.; de Castro, H.F.; Da Ros, P.C.M.; Mendes, A.A.; Giordano, R.L.C.; Tardioli, P.W. Immobilization of *Pseudomonas fluorescens* lipase on hydrophobic supports and application in biodiesel synthesis by transesterification of vegetable oils in solvent-free systems. *J. Ind. Microbiol. Biotechnol.* **2015**, *42*, 523–535. [[CrossRef](#)] [[PubMed](#)]
13. Zniszczol, A.; Herman, A.P.; Szymanska, K.; Mrowiec-Bialon, J.; Walczak, K.Z.; Jarzebski, A.; Boncel, S. Covalently immobilized lipase on aminoalkyl-, carboxy- and hydroxy-multi-wall carbon nanotubes in the enantioselective synthesis of Solketal esters. *Enzyme Microb. Technol.* **2016**, *87*, 61–69. [[CrossRef](#)] [[PubMed](#)]
14. Krajewska, B. Application of chitin- and chitosan-based materials for enzyme immobilizations: A review. *Enzyme Microb. Technol.* **2004**, *35*, 126–139. [[CrossRef](#)]
15. Mendes, A.A.; de Castro, H.F.; Rodrigues, D.S.; Adriano, W.S.; Tardioli, P.W.; Mammarella, E.J.; Giordano, R.C.; Giordano, R.L.C. Multipoint covalent immobilization of lipase on chitosan hybrid hydrogels: Influence of the polyelectrolyte complex type and chemical modification on the catalytic properties of the biocatalysts. *J. Ind. Microbiol. Biotechnol.* **2011**, *38*, 1055–1066. [[CrossRef](#)] [[PubMed](#)]
16. Dos Santos, J.C.S.; Barbosa, O.; Ortiz, C.; Berenguer-Murcia, A.; Rodrigues, R.C.; Fernandez-Lafuente, R. Importance of the support properties for immobilization or purification of enzymes. *ChemCatChem* **2015**, *7*, 2413–2432. [[CrossRef](#)]
17. Cicolatti, E.P.; Valério, A.; Henriques, R.O.; Moritz, D.E.; Ninow, J.L.; Freire, D.M.G.; Manoel, E.A.; Fernandez-Lafuente, R.; De Oliveira, D. Nanomaterials for biocatalyst immobilization—state of the art and future trends. *RSC Adv.* **2016**, *6*, 104675–104692. [[CrossRef](#)]
18. Fernandez-Lafuente, R.; Armisen, P.; Sabuquillo, P.; Fernández-Lorente, G.; Guisán, J.M. Immobilization of lipases by selective adsorption on hydrophobic supports. *Chem. Phys. Lipids* **1998**, *93*, 185–197. [[CrossRef](#)]
19. Manoela, E.A.; dos Santos, J.C.S.; Freire, D.M.G.; Rueda, N.; Fernández-Lafuente, R. Immobilization of lipases on hydrophobic supports involves the open form of the enzyme. *Enzyme Microb. Technol.* **2015**, *71*, 53–57. [[CrossRef](#)] [[PubMed](#)]
20. Kilinc, A.; Teke, M.; Onal, S.; Telefoncu, A. Immobilization of pancreatic lipase on chitin and chitosan. *Prep. Biochem. Biotechnol.* **2006**, *36*, 153–163. [[CrossRef](#)] [[PubMed](#)]
21. Gomes, F.M.; Pereira, E.B.; de Castro, H.F. Immobilization of lipase on chitin and its use in nonconventional biocatalysis. *Biomacromolecules* **2004**, *5*, 17–23. [[CrossRef](#)] [[PubMed](#)]
22. Rattanaphra, D.; Srinophakun, P. Biodiesel production from crude sunflower oil and crude jatropha oil using immobilized lipase. *J. Chem. Eng. Jpn.* **2010**, *43*, 104–108. [[CrossRef](#)]
23. Wang, Z.G.; Wang, J.Q.; Xu, Z.K. Immobilization of lipase from *Candida rugosa* on electrospun polysulfone nanofibrous membranes by adsorption. *J. Mol. Catal. B: Enzym.* **2006**, *42*, 45–51. [[CrossRef](#)]
24. Chen, Z.; Xu, W.; Jin, L.; Zha, J.; Tao, T.; Lin, Y.; Wang, Z. Synthesis of amine-functionalized Fe<sub>3</sub>O<sub>4</sub>@C nanoparticles for lipase immobilization. *J. Mater. Chem. A* **2014**, *2*, 18339–18344. [[CrossRef](#)]
25. Hou, C.; Zhou, L.; Zhu, H.; Wang, X.; Hu, N.; Zeng, F.; Wang, L.; Yin, H. Mussel-inspired surface modification of magnetic@graphite nanosheets composite for efficient *Candida rugosa* lipase immobilization. *J. Ind. Microbiol. Biotechnol.* **2015**, *42*, 723–734. [[CrossRef](#)] [[PubMed](#)]
26. Magner, E. Immobilisation of enzymes on mesoporous silicate materials. *Chem. Soc. Rev.* **2013**, *42*, 6213–6222. [[CrossRef](#)] [[PubMed](#)]
27. Le, D.M.; Sorensen, H.R.; Knudsen, N.O.; Meyer, A.S. Implications of silica on biorefineries—Interactions with organic material and mineral elements in grasses. *Biofuels Bioprod. Biorefin.* **2015**, *9*, 109–121. [[CrossRef](#)]
28. Szymanska, K.; Odrozek, K.; Zniszczol, A.; Torrelo, G.; Resch, V.; Hanefeld, U.; Jarzebski, A.B. MsAcT in siliceous monolithic microreactors enables quantitative ester synthesis in water. *Catal. Sci. Technol.* **2016**, *6*, 4882–4888. [[CrossRef](#)]

29. Szymanska, K.; Pietrowska, M.; Kocurek, J.; Maresz, K.; Koreniuk, A.; Mrowiec-Białon, J.; Widlak, P.; Magner, E.; Jarzebski, A. Low back-pressure hierarchically structured multichannel microfluidic bioreactors for rapid protein digestion—Proof of concept. *Chem. Eng. J.* **2016**, *287*, 148–154. [[CrossRef](#)]
30. Yu, W.H.; Tong, D.S.; Fang, M.; Shao, P.; Zhou, C.H. Cloning, expression and enzymatic characterization of an aldo-keto reductase from *Candida albicans* XP1463. *J. Mol. Catal. B: Enzym.* **2015**, *111*, 43–50. [[CrossRef](#)]
31. Zou, B.; Hu, Y.; Yu, D.; Jiang, L.; Liu, W.; Song, P. Functionalized ionic liquid modified mesoporous silica SBA-15: A novel, designable and efficient carrier for porcine pancreas lipase. *Colloids Surf. B: Biointerfaces* **2011**, *88*, 93–99. [[CrossRef](#)] [[PubMed](#)]
32. Gao, S.; Wang, Y.; Diao, X.; Luo, G.; Dai, Y. Effect of pore diameter and cross-linking method on the immobilization efficiency of *Candida rugosa* lipase in SBA-15. *Bioresour. Technol.* **2010**, *101*, 3830–3837. [[CrossRef](#)] [[PubMed](#)]
33. Thakur, V.K.; Thakur, M.K. Recent advances in green hydrogels from lignin: A review. *Int. J. Biol. Macromol.* **2015**, *72*, 834–847. [[CrossRef](#)] [[PubMed](#)]
34. Thakur, V.K.; Thakur, M.K.; Raghavan, P.; Kessler, M.R. Progress in green polymer composites from lignin for multifunctional applications: A review. *ACS Sustain. Chem. Eng.* **2015**, *2*, 1072–1092. [[CrossRef](#)]
35. Zdarta, J.; Klapiszewski, L.; Wysokowski, M.; Norman, M.; Kołodziejczak-Radzimska, A.; Moszyński, D.; Ehrlich, H.; Maciejewski, H.; Stelling, A.L.; Jesionowski, T. Chitin-lignin material as a novel matrix for enzyme immobilization. *Mar. Drugs* **2015**, *13*, 2424–2446. [[CrossRef](#)] [[PubMed](#)]
36. Klapiszewski, L.; Nowacka, M.; Milczarek, G.; Jesionowski, T. Physicochemical and electrokinetic properties of silica/lignin biocomposites. *Carbohydr. Polym.* **2013**, *94*, 345–355. [[CrossRef](#)] [[PubMed](#)]
37. Jesionowski, T.; Klapiszewski, L.; Milczarek, G. Kraft lignin and silica as precursors of advanced composite materials and electroactive blends. *J. Mater. Sci.* **2014**, *49*, 1376–1385. [[CrossRef](#)]
38. Hou, J.; Dong, G.; Ye, Y.; Chen, V. Enzymatic degradation of bisphenol-A with immobilized laccase on TiO<sub>2</sub> sol-gel coated PVDF membrane. *J. Membr. Sci.* **2014**, *469*, 19–30. [[CrossRef](#)]
39. Zdarta, J.; Sałek, K.; Kołodziejczak-Radzimska, A.; Siwińska-Stefańska, K.; Szwarc-Rzepka, K.; Norman, M.; Klapiszewski, L.; Bartczak, P.; Kaczorek, E.; Jesionowski, T. Immobilization of *Amano Lipase A* onto Stöber silica surface: Process characterization and kinetic studies. *Open Chem.* **2015**, *13*, 138–148. [[CrossRef](#)]
40. Souza, R.L.; Resende, W.C.; Barao, C.E.; Zanin, G.M.; de Castro, H.F.; Santos, O.A.A.; Fricks, A.T.; Figueiredo, R.T.; Lima, Á.S.; Soares, C.M.F. Influence of the use of Aliquat 336 in the immobilization procedure in sol-gel of lipase from *Bacillus* sp. ITP-001. *J. Mol. Catal. B: Enzym.* **2012**, *84*, 152–159. [[CrossRef](#)]
41. Gao, Z.; Zhan, W.; Guo, Y.; Wang, Y.; Guo, Y.; Lu, G. Aldehyde propyl-functionalized mesostructured cellular foams: Efficient supports for immobilization of penicillin G acylase. *J. Mol. Catal. B: Enzym.* **2014**, *105*, 111–117. [[CrossRef](#)]
42. Wong, P.T.T.; Nong, R.K.; Caputo, T.A.; Godwin, T.A.; Rigas, B. Infrared spectroscopy of exfoliated human cervical cells: Evidence of extensive structural changes during carcinogenesis. *Proc. Natl. Acad. Sci. USA* **1991**, *88*, 10988–10992. [[CrossRef](#)] [[PubMed](#)]
43. Portaccio, M.; Della Ventura, B.; Mita, D.G.; Manolova, N.; Stoilova, O.; Rashkov, I.; Lepore, M. FT-IR microscopy characterization of sol-gel layers prior and after glucose oxidase immobilization for biosensing applications. *J. Sol-Gel Sci. Technol.* **2011**, *57*, 204–211. [[CrossRef](#)]
44. Jesionowski, T.; Krysztafkiwicz, A. Comparison of the techniques used to modify amorphous hydrated silicas. *J. Non-Cryst. Solids* **2000**, *277*, 45–57. [[CrossRef](#)]
45. Tomizuka, N.; Ota, Y.; Yamada, K. Lipase from *Candida cylindracea* II. Amino acid composition, carbohydrate component, and some physical properties. *Agric. Biol. Chem.* **1966**, *30*, 1090–1096.
46. Klapiszewski, L.; Bartczak, P.; Wysokowski, M.; Jankowska, M.; Kabat, K.; Jesionowski, T. Silica conjugated with kraft lignin and its use as a novel ‘green’ sorbent for hazardous metal ions removal. *Chem. Eng. J.* **2015**, *260*, 684–693. [[CrossRef](#)]
47. Ghosh, T.; Sarkar, P.; Turner, A.P.F. A novel third generation uric acid biosensor using uricase electro-activated with ferrocene on a Nafion coated glassy carbon electrode. *Bioelectrochemistry* **2015**, *102*, 1–9. [[CrossRef](#)] [[PubMed](#)]
48. Jeyapragasam, T.; Saraswathi, R. Electrochemical biosensing of carbofuran based on acetylcholinesterase immobilized onto iron oxide-chitosan nanocomposite. *Sens. Actuators B: Chem.* **2014**, *191*, 681–687. [[CrossRef](#)]

49. Wysokowski, M.; Klapiszewski, Ł.; Moszyński, D.; Bartczak, P.; Szatkowski, T.; Majchrzak, I.; Siwińska-Stefańska, K.; Bazhenov, V.V.; Jesionowski, T. Modification of chitin with kraft lignin and development of new biosorbents for removal of cadmium(II) and nickel(II) ions. *Mar. Drugs* **2014**, *12*, 2245–2268. [[CrossRef](#)] [[PubMed](#)]
50. Stevens, J.S.; Luca, A.C.; Pelendritis, M.; Terenghi, G.; Downes, S.; Schroeder, S.L.M. Quantitative analysis of complex amino acids and RGD peptides by X-ray photoelectron spectroscopy (XPS). *Surf. Interface Anal.* **2013**, *45*, 1238–1246. [[CrossRef](#)]
51. Peirce, S.; Tacias-Pascacio, V.G.; Russo, M.E.; Marzocchella, A.; Virgen-Ortiz, J.J.; Fernandez-Lafuente, R. Stabilization of *Candida antarctica* lipase B (CALB) immobilized on octyl agarose by treatment with polyethyleneimine (PEI). *Molecules* **2016**, *21*, 751–765. [[CrossRef](#)] [[PubMed](#)]
52. Svendsen, A. Lipase protein engineering. *Biochim. Biophys. Acta* **2000**, *1543*, 223–238. [[CrossRef](#)]
53. Milczarek, G.; Ignatas, O. Renewable cathode materials from biopolymer/conjugated polymer interpenetrating networks. *Science* **2012**, *335*, 1468–1471. [[CrossRef](#)] [[PubMed](#)]
54. Jesionowski, T.; Klapiszewski, Ł.; Milczarek, G. Structural and electrochemical properties of multifunctional silica/lignin materials. *Mater. Chem. Phys.* **2014**, *147*, 1049–1057. [[CrossRef](#)]
55. Zhang, R.; Xiao, X.; Tai, Q.; Huang, H.; Yang, J.; Hu, Y. Preparation of lignin-silica hybrids and its application in intumescent flame-retardant poly(lactic acid) system. *High Perform. Polym.* **2012**, *24*, 738–745. [[CrossRef](#)]
56. Mateo, C.; Abian, O.; Fernandez-Lorente, G.; Pedroche, J.; Fernandez-Lafuente, R.; Guisan, J.M. Epoxy sepabeads: A novel epoxy support for stabilization of industrial enzymes via very intense multipoint covalent attachment. *Biotechnol. Prog.* **2002**, *18*, 629–634. [[CrossRef](#)] [[PubMed](#)]
57. Mateo, C.; Torres, R.; Fernandez-Lorente, G.; Ortiz, C.; Fuentes, M.; Hidalgo, A.; Lopez-Gallego, F.; Abian, O.; Palomo, J.M.; Betancor, L.; et al. Epoxy-amino groups: A new tool for improved immobilization of proteins by the epoxy method. *Biomacromolecules* **2003**, *4*, 772–777. [[CrossRef](#)] [[PubMed](#)]
58. Sheldon, R.A.; van Pelt, S. Enzyme immobilisation in biocatalysis: Why, what and how? *Chem. Soc. Rev.* **2013**, *42*, 6223–6235. [[CrossRef](#)] [[PubMed](#)]
59. Forsyth, C.; Patwardhan, S.V. Controlling performance of lipase immobilised on bioinspired silica. *J. Mater. Chem. B* **2013**, *1*, 1164–1174. [[CrossRef](#)]
60. Emregul, E.; Sungur, S.; Akbulut, U. Polyacrylamide-gelatine carrier system used for invertase immobilization. *Food Chem.* **2006**, *97*, 591–597. [[CrossRef](#)]
61. Dong, L.; Ge, C.; Qin, P.; Chen, Y.; Xu, Q. Immobilization and catalytic properties of *Candida lipolytic* lipase on surface of organic intercalated and modified MgAl-LDHs. *Solid State Sci.* **2014**, *31*, 8–15. [[CrossRef](#)]
62. Xie, W.; Wang, J. Enzymatic production of biodiesel from soybean oil by using immobilized lipase on Fe<sub>3</sub>O<sub>4</sub>/poly(styrene-methacrylic acid) magnetic microsphere as a biocatalyst. *Energy Fuels* **2014**, *28*, 2624–2631. [[CrossRef](#)]
63. Tutarb, H.; Yilmaza, E.; Pehlivan, E.; Yilmaz, M. Immobilization of *Candida rugosa* lipase on sporopollenin from *Lycopodium clavatum*. *Int. J. Biol. Macromol.* **2009**, *4*, 315–320. [[CrossRef](#)] [[PubMed](#)]
64. Abdel-Naby, M.A. Immobilization of *Aspergillus niger* NRC 107 xylanase and beta-xylosidase, and properties of the immobilized enzymes. *Appl. Biochem. Biotechnol.* **1993**, *38*, 69–81. [[CrossRef](#)] [[PubMed](#)]
65. Narwal, S.K.; Saun, N.K.; Gupta, R. Characterization and catalytic properties of free and silica-bound lipase: A comparative study. *J. Oleo Sci.* **2014**, *63*, 599–605. [[CrossRef](#)] [[PubMed](#)]
66. Gupta, P.; Rouf, A.; Shahb, B.A.; Mahajana, N.; Chaubey, A.; Tanejaba, S.C. *Arthrobacter* sp. lipase catalyzed kinetic resolution of BINOL: The effect of substrate immobilization. *J. Mol. Catal. B: Enzym.* **2014**, *101*, 35–39. [[CrossRef](#)]
67. Zivkovic, L.T.I.; Zivkovic, L.S.; Babic, B.M.; Kokunesoski, M.J.; Jokic, B.M.; Karadzic, I.M. Immobilization of *Candida rugosa* lipase by adsorption onto biosafe meso/macroporous silica and zirconia. *Biochem. Eng. J.* **2015**, *93*, 73–83. [[CrossRef](#)]
68. Ho, L.J.; Lee, D.H.; Lim, J.S.; Um, B.H.; Park, C.; Kang, S.W.; Kim, S.W. Optimization of the process for biodiesel production using a mixture of immobilized *Rhizopus oryzae* and *Candida rugosa* lipases. *J. Microbiol. Biotechnol.* **2008**, *18*, 1927–1931.
69. Chen, Y.; Liu, J.; Xia, C.; Zhao, C.; Ren, Z.; Zhang, W. Immobilization of lipase on porous monodisperse chitosan microspheres. *Biotechnol. Appl. Biochem.* **2014**, *62*, 101–106. [[CrossRef](#)] [[PubMed](#)]



70. Zhu, Y.T.; Ren, X.Y.; Liu, Y.M.; Wei, Y.; Qing, L.S.; Liao, X. Covalent immobilization of porcine pancreatic lipase on carboxyl-activated magnetic nanoparticles: Characterization and application for enzymatic inhibition assays. *Mater. Sci. Eng.: C* **2014**, *38*, 278–285. [[CrossRef](#)] [[PubMed](#)]
71. Ansari, S.A.; Husain, Q. Potential applications of enzymes immobilized on/in nano materials: A review. *Biotechnol. Adv.* **2012**, *30*, 512–523. [[CrossRef](#)] [[PubMed](#)]
72. Wang, X.Y.; Jiang, X.P.; Li, Y.; Zeng, S.; Zhang, Y.W. Preparation Fe<sub>3</sub>O<sub>4</sub>@chitosan magnetic particles for covalent immobilization of lipase from *Thermomyces lanuginosus*. *Int. J. Biol. Macromol.* **2015**, *75*, 44–50. [[CrossRef](#)] [[PubMed](#)]
73. Krysztafkiewicz, A.; Rager, B.; Jesionowski, T. The effect of surface modification on physicochemical properties of precipitated silica. *J. Mater. Sci.* **1997**, *32*, 1333–1339. [[CrossRef](#)]
74. Jesionowski, T.; Ciesielczyk, F.; Krysztafkiewicz, A. Influence of selected alkoxysilanes on dispersive properties and surface chemistry of spherical silica precipitated in emulsion media. *Mater. Chem. Phys.* **2010**, *119*, 65–74. [[CrossRef](#)]
75. Klapiszewski, L.; Zdarta, J.; Szatkowski, T.; Wysokowski, M.; Nowacka, M.; Szwarc-Rzepka, K.; Bartczak, P.; Siwińska-Stefańska, K.; Ehrlich, H.; Jesionowski, T. Silica/lignosulfonate hybrid materials: Preparation and characterization. *Cent. Eur. J. Chem.* **2014**, *12*, 719–735. [[CrossRef](#)]
76. Horcas, I.; Fernandez, R.; Gomez-Rodriguez, J.M.; Colchero, J.; Gomez-Herrero, J.; Baro, A.M. WSXM: A software for scanning probe microscopy and a tool for nanotechnology. *Rev. Sci. Instrum.* **2007**, *78*, 013705. [[CrossRef](#)] [[PubMed](#)]



© 2016 by the authors; licensee MDPI, Basel, Switzerland. This article is an open access article distributed under the terms and conditions of the Creative Commons Attribution (CC-BY) license (<http://creativecommons.org/licenses/by/4.0/>).